



# Description and evaluation of airborne microplastics in the United Kingdom Earth System Model (UKESM1.1) using GLOMAP-mode

Cameron McErlich<sup>1</sup>, Felix Goddard<sup>1</sup>, Alex Aves<sup>1</sup>, Catherine Hardacre<sup>1</sup>, Nikolaos Evangeliou<sup>2</sup>, and Laura E. Revell<sup>1</sup>

<sup>1</sup>School of Physical and Chemical Sciences, University of Canterbury, Christchurch, New Zealand

Correspondence: Cameron McErlich (cameron.mcerlich@canterbury.ac.nz); Laura Revell (laura.revell@canterbury.ac.nz)

Abstract. Airborne microplastics are a recently identified atmospheric aerosol species with potential air quality and climate impacts, yet they are not currently represented in global climate models. Here, we describe the addition of microplastics to the aerosol scheme of the UK Earth System Model (UKESM1.1): the Global Model of Aerosol Processes (GLOMAP). Microplastics are included as both fragments and fibres across a range of aerosol size modes, enabling interaction with existing aerosol processes such as ageing and wet and dry deposition. Simulated microplastics have higher concentrations over land, but can be transported into remote regions including Antarctica despite no assumed emissions from these regions. Lifetimes range between ~17 days to ~1 hour, with smaller, soluble microplastics having longer lifetimes. Microplastics are well-mixed throughout the troposphere, and the smallest particles are simulated to reach the lower stratosphere in small numbers. Dry deposition is the dominant microplastic removal pathway, but greater wet deposition occurs for smaller soluble microplastic, due to interactions with clouds. Although microplastics currently contribute a minor fraction of the total aerosol burden, their concentration is expected to increase in future if plastic production continues to increase, and as existing plastic waste in the environment degrades to form new microplastic. Incorporating microplastics into UKESM1.1 is a key step toward quantifying their current atmospheric impact and offers a framework for simulating future emission scenarios for an assessment of their long term impacts on air quality and climate.

## 15 1 Introduction

Since large-scale plastic production began over the  $20^{\rm th}$  century, plastics have become the most used synthetic material in the world due to their versatility and durability. However, plastics become brittle as they age and break down through exposure to sunlight and other environmental factors (Gewert et al., 2015). This degradation forms microplastics (plastic particles 1-5000  $\mu$ m) and nanoplastics (particles smaller than 1  $\mu$ m), which have the potential to cause ecological damage (MacLeod et al., 2021). It is estimated that 5 Gt of plastic waste has accumulated in landfills and the natural environment since the 1950s, and that unless serious changes are made to curb global plastic production and management the abundance of plastic litter will double over the next 30 years (Geyer et al., 2017).

<sup>&</sup>lt;sup>2</sup>Stiftelsen NILU (former Norwegian Institute for Air Research), Department of Atmospheric and Climate Research (ATMOS), Kjeller, Norway





Microplastics have long been studied in the marine environment (Carpenter et al., 1972; Carpenter and Smith, 1972), where they are ingested by marine organisms, causing physical harm and disrupting feeding behaviour (Kvale et al., 2021). Since the first study of microplastics in atmospheric fallout (Dris et al., 2015), many further reports of airborne microplastics have been published (e.g. Allen et al., 2022, and references therein). Due to their small size and low densities, microplastics are transported throughout the atmosphere (Evangeliou et al., 2020). In particular, studies carried out in the Arctic (Bergmann et al., 2019), Antarctic (Aves et al., 2022) and other remote locations (Brahney et al., 2020; Allen et al., 2021; Materić et al., 2021) indicate that airborne microplastics are ubiquitous.

As a form of atmospheric aerosol, microplastics can contribute to climate change by interacting with incoming solar and outgoing thermal radiation. This in turn has an impact on the radiative balance of the atmosphere (Revell et al., 2021). Aerosols such as microplastics can also have indirect effects on radiative balance through cloud interactions and by acting as cloud condensation nuclei (CCN) (Aeschlimann et al., 2022). Clouds play an important role in the climate system (Forster et al., 2021) by reflecting sunlight to space (which has a cooling effect on Earth's surface) and trapping thermal radiation emitted by the Earth (which has a warming effect). In general, clouds that have been perturbed by aerosols consist of more numerous and smaller cloud droplets, so that they reflect more sunlight and are longer lived (Twomey, 1977; Albrecht, 1989).

Although the field of airborne microplastic-climate interactions is in its infancy, several lines of evidence from field and lab studies demonstrate that microplastic-cloud interactions occur. Microplastics are present throughout the lower atmosphere at cloud-forming altitudes, having been found as high as 3500 m above sea level (Allen et al., 2021; González-Pleiter et al., 2021). Microplastics have also been collected in cloud water (Xu et al., 2024; Wang et al., 2023), indicating their uptake into clouds occurs and that microplastics potentially act as cloud condensation nuclei (CCN). Studies have also determined that microplastics can act as ice nucleating particles (INP) when pristine and when aged through environmental processes such as exposure to ultraviolet light and ozone. (Ganguly and Ariya, 2019; Busse et al., 2024; Brahana et al., 2024; Seifried et al., 2024). If present in high enough concentration, this indicates that microplastics can potentially seed cloud formation. Research remains conflicted about how the ageing impacts the nucleation ability of microplastics, with studies indicating both increases (Brahana et al., 2024) and decreases (Busse et al., 2024; Seifried et al., 2024) in the ice nucleation activity of microplastics due to ageing. Tatsii et al. (2025) found when modelling atmospheric microplastics under high emissions scenarios they can potentially contribute significantly to INP concentrations.

The contribution of airborne microplastics to global aerosol loading and implications for climate change are not well understood, since global climate models do not include microplastics in their aerosol schemes. Here we describe the addition of microplastics as a new aerosol species to the United Kingdom Earth System Model. The model and the microplastics scheme are described in Section 2. In Section 3 we present simulations of the global airborne microplastics loading and deposition to the marine and terrestrial environments. We also evaluate the model against current observational data.





## 2 Methods

60

## 2.1 Model description

Model simulations were performed using the UK Earth System Model at version 1.1 (UKESM1.1). UKESM1.1 is built on component models which each simulate a domain of the Earth system including the physical atmosphere, atmospheric composition and chemistry, ocean, sea ice and the land surface. Additional Earth system processes included in UKESM1.1 are ocean biogeochemistry and terrestrial biogeochemistry. The UKESM1.1 component models are coupled together to capture the climate impact of interactions and feedbacks within the Earth system. UKESM1.1 operates on a grid with a resolution of 1.25° latitude × 1.85° longitude, and the atmosphere contains 85 unevenly spaced levels extending to 85 km above the surface. The fully coupled configuration of UKESM1.1 (and the earlier UKESM1 version) is described in Sellar et al. (2019); Mulcahy et al. (2023).

Here we use the atmosphere only UKESM1.1 configuration, UKESM1.1-AMIP, as we are primarily interested in the atmospheric transport of microplastics. Like the fully coupled configuration, the physical atmosphere component of UKESM1.1 is the Global Atmosphere 7.1 (GA7.1) science configuration of the Unified Model (Walters et al., 2019; Mulcahy et al., 2018). Atmospheric composition, chemistry and aerosols are simulated by the United Kingdom Chemistry and Aerosols (UKCA) model (Archibald et al., 2020) coupled with the two-moment modal aerosol microphysics scheme, the Global Model of Aerosol Processes (GLOMAP; Mulcahy et al. 2020). In UKESM1.1-AMIP the physical atmosphere and the atmospheric composition are coupled, but sea surface temperature, ocean biogeochemistry, sea ice, land surface, terrestrial biogeochemistry are prescribed from a fully coupled UKESM1.1 simulation.

In UKESM1.1, UKCA uses a combined stratospheric and tropospheric chemistry scheme within. The 'StratTrop' scheme simulates interactive chemistry from the surface to the top of the model and describes the chemistry of 81 species through 291 thermal and photolytic reactions (Archibald et al., 2020). GLOMAP currently simulates the number and mass balances across six aerosol species, modelling their sources, sinks and evolution. Aerosol species in GLOMAP include sulfate (SO<sub>4</sub>), black carbon (BC), organic matter (OM), sea salt, dust, and nitrate (Mann et al., 2010; Jones et al., 2021). Aerosol species are represented in eight log-normal size modes: nucleation soluble mode, Aitken soluble mode, accumulation soluble mode, coarse soluble mode, Aitken insoluble mode, accumulation insoluble mode, coarse insoluble mode and super-coarse insoluble mode (Mulcahy et al., 2020). These modes, their sizes ranges and represented aerosol species in each mode are summarised in Table 1. Aerosols in the soluble modes can be incorporated into cloud droplets and affect the formation of clouds; Typically aerosols with a radius of  $\geq 25$  nm are activated into CCN and cloud droplets (Abdul-Razzak and Ghan, 2000; Walters et al., 2019). Aerosols in the insoluble modes do not act as CCN. Aerosol species can settle out of the atmosphere through dry deposition and wet deposition processes such as nucleation scavenging (rainout), impaction scavenging (washout), and convective plume scavenging.





The UKESM1.1 radiative transfer scheme uses the Suite of Community Radiative Transfer codes based on Edwards and Slingo (SOCRATES; Edwards and Slingo, 1996). The shortwave part of the spectrum between 200 nm and 10 µm is divided into six spectral bands and the longwave part between 3.3 µand 1 cm into nine spectral bands. Direct aerosol-radiation interactions are calculated in UKCA by the RADAER component of GLOMAP (Bellouin, 2010). This determines aerosol optical properties via Mie theory which are passed to the model radiation scheme to interactively calculate scattering and absorption of radiation by aerosol species. This requires tabulations of the complex refractive index of each aerosol species across the model spectral bands.

41	n	n

Mode name	Diameter range	Represented Aerosols
Nucleation Soluble	< 5 nm	SO <sub>4</sub> , OC
Aitken Soluble	5-50  nm	$SO_4$ , BC, OC, $NO_3$ , MP
Aitken Insoluble	5-50  nm	BC, OC, MP
Accumulation Soluble	$50-250~\mathrm{nm}$	$SO_4$ , BC, OC, SS, DU, $NO_3$ , MP
Accumulation Insoluble	50 - 500  nm	DU, MP
Coarse Soluble	$>250~\mathrm{nm}$	SO <sub>4</sub> , BC, OC, SS, DU, NH <sub>4</sub> , NO <sub>3</sub> , MP
Coarse Insoluble	> 500 nm	DU, MP
Super-coarse Insoluble	$> 2500 \; \mathrm{nm}$	DU, MP

**Table 1.** Description of the eight log-normal size modes in GLOMAP and aerosol species represented in each mode. Current species are sulphate (SO<sub>4</sub>) in the form of sulphuric acid, black carbon (BC), organic carbon (OC) in the form of organic matter (OM) with an OM:OC ratio of 1:4, sea salt (SS), nitrate (NO<sub>3</sub>; in the form of ammonium nitrate in the Aitken and accumulation soluble modes, and in the form of sodium nitrate in the accumulation and coarse soluble modes), dust (DU). The new microplastic aerosol species (*MP*) is represented in all modes except the nucleation mode, (see Section 2.4).

# 2.2 Microplastic emissions

Microplastic emissions are difficult to estimate globally due to a lack of consistent measurements with good spatial coverages. Microplastics are emitted into UKESM1.1 using an updated version of the observationally-derived inventory from Evangeliou et al. (2022). Microplastics are emitted in two different shapes of fragments and fibres. Microplastic fragments are small pieces of plastic created through the deterioration of larger plastic pieces (macroplastics), whereas microplastic fibres are thread like plastics primarily produced from clothing and other fabrics. In the original emissions inventory of Evangeliou et al. (2022), microplastic fragments are represented in five size bins between diameters of  $5 - 250 \,\mu\text{m}$ , and microplastic fibres are represented



125



in nine size bins with lengths between  $10-3000~\mu m$  and widths between  $1-10~\mu m$ .

The microplastic inventory is based on airborne microplastic deposition measurements collected across 11 National Park and Wilderness sites between 2017 and 2019 in the Western USA (Brahney et al., 2020). Sources of the fallout measurements were determined using the FLEXPART particle dispersion model running in retroplume mode to calculate back trajectories. These sources were combined with a robust Bayesian inverse modelling algorithm to determine microplastic emissions, and then extrapolated globally using inventories of other emissions. Sea salt, agriculture, mineral dust and road dust were used as the main sources of microplastic fragments. For the microplastic fibres, their main source was assumed to be largely from clothing and linked to the distribution of the global population.

Since the original publication, updates have been made to the emissions inventory, which are accounted for in this study. The updated inventory now considers the positions of ocean gyres when determining oceanic microplastic emissions (Isobe et al., 2021). The high emissions observed across polar regions in Evangeliou et al. (2022) have been reduced, and emissions over land have been increased. To create emissions data files for UKESM1.1-AMIP the updated inventory was re-gridded with a resolution of 1.25° latitude × 1.85° longitude. One year of emissions data is available for 2018, based on when the airborne microplastic deposition measurements were collected (Brahney et al., 2020). Figure 1 shows microplastics emissions for both fragments and fibres using the updated emissions inventory.

# 2.3 Extrapolation of microplastic emissions

As indicated by the size ranges of the insoluble GLOMAP modes in Table 1, all of the microplastics emissions from Evangeliou et al. (2022), i.e. sizes greater than 5 µm, correspond to the super-coarse insoluble mode which has a lower bound of 2.5 µm diameter and no upper bound. To input emissions into the smaller Aitken, accumulation and coarse insoluble modes, microplastic fragment emissions were extrapolated. This extrapolation was based on methodology described by Leusch et al. (2023), which surveyed more than 120 published studies reporting microplastic size distributions and identified a power law distribution which was common across several matrices (air, water, soil); exponentially larger numbers of particles are found at smaller sizes. When log-transformed, Leusch et al. (2023) demonstrate a linear increase in particle number with decreasing size. Leusch et al. (2023) further demonstrated that if the concentration of microplastics in a particular size bin is known, then the concentration in a different size bin can be estimated using Equation 1:

$$n_{pred} = n_{ref} \times \left(\frac{x_{UB.pred} - x_{LB.pred}}{x_{UB.ref} - x_{LB.ref}}\right) \times \left(\frac{x_{UB.pred} \times x_{LB.pred}}{x_{UB.ref} \times x_{LB.ref}}\right)^{-\alpha/2} \tag{1}$$





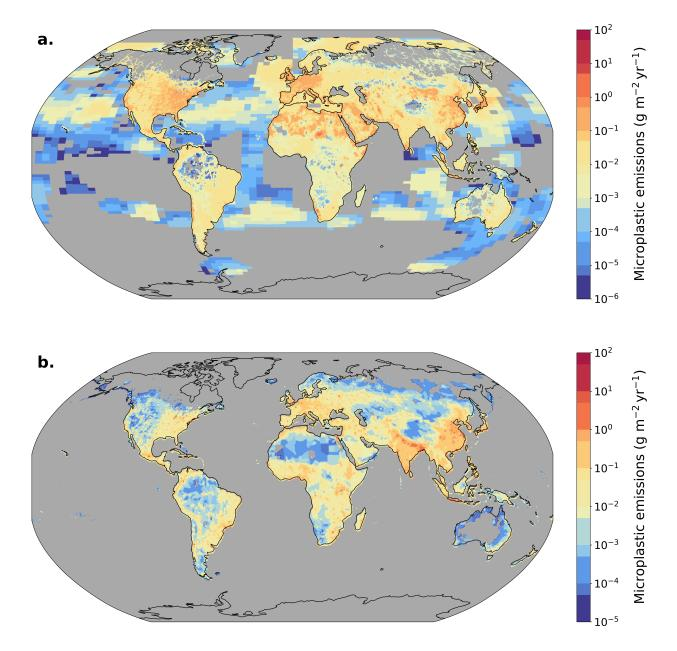


**Figure 1.** The microplastic emissions inventory for (a) microplastic fragments and (b) microplastic fibres, updated from Evangeliou et al (2022). Grey shading indicates that emissions are zero.

Where  $n_{pred}$  is the number of microplastics predicted in a size bin with upper and lower bounds  $x_{UB.pred}$  and  $x_{LB.pred}$ , respectively.  $n_{ref}$  is the number of microplastics in the reference bin with upper and lower bounds  $x_{UB.ref}$  and  $x_{LB.ref}$ , respectively.  $\alpha$  is the slope of the linear regression of the log-logistic fit.



165

170

175



Microplastic fragments were extrapolated using the  $10-25~\mu m$  bin as a reference because it contained the largest number of microplastics. The value of  $\alpha$  was tuned to provide the best match between the extrapolated data and the remaining four bins for microplastics fragments with emissions data.  $\alpha$  was chosen to be 1.81 which matches the reference values of  $1.44\pm0.37$  given for airborne microplastics in Leusch et al. (2023). Supplementary Figure A1 shows the results of the extrapolation, for both the number and mass concentration of microplastics. The extrapolated estimates of microplastic fragments are only used across the size bins where observationally-derived microplastic data is absent. Extrapolation of the microplastic fragments to the GLOMAP size modes indicated in Table 2 extends their representation into the nanometer size range. While these particles fall within the definition of nanoplastics, they are referred to as microplastics throughout this study for clarity. Microplastic fibres were not extrapolated due to their thread like shape; Once the length of microplastic fibres approaches the nanometre range their aspect ratios (length/diameter) become small enough they essentially behave more as microplastic fragments.

# 2.4 Implementation of microplastics into GLOMAP

Microplastics have been added to GLOMAP in a new aerosol configuration that also includes sulfate, black carbon, organic matter, sea salt and dust. This allows interactions between microplastics and the other aerosol species. Microplastics are emitted into the insoluble Aitken, accumulation, coarse and super-coarse modes. However, microplastics can be transferred to the soluble modes through an ageing process of aerosol species previously existing within GLOMAP. This ageing occurs due to a build-up of soluble material such as sulfate on the surface of the aerosol (Mulcahy et al., 2018). Once the soluble material builds up to a size of 10 monolayers, the aerosol particles are transferred to the corresponding soluble mode. This effectively allows them to act as CCN as they remain aloft in the atmosphere. Because the model does not contain a super-coarse soluble mode, there is no transfer of microplastics from the super-coarse insoluble mode to a corresponding soluble mode. Similar to other aerosol species in GLOMAP, microplastics are also able to undergo wet and dry deposition, and are able to coagulate.

Atmospheric transport and lifetime of microplastic fibres is influenced by their shapes (Tatsii et al., 2024; Xiao et al., 2023). Because of their non-spherical shape, microplastic fibres may be transported higher into the atmosphere than microplastic fragments. Tatsii et al. (2024) concluded that microplastic fibres have settling velocities up to 76% lower when compared to spheres of an equivalent volume. This suggests microplastic fibres need to be treated differently within the model, however they currently have the same spherical shape and settling velocities as the microplastic fragments.

Microplastic fragments and fibres can be switched off separately, allowing for model runs with both, one or neither of the two types enabled. While current representation of microplastic fibres may not be realistic, the partitioning between fragment and fibre emissions creates a separate framework for microplastic fibres that future iterations of the microplastic scheme can improve upon. The direct radiative effects of microplastics are included via RADAER. We use the complex refractive index of Revell et al. (2021) for colourless plastics, such that all plastics are treated as colourless. Note that, as RADAER calculates aerosol radiative effects using Mie theory, all microplastic particles are assumed to be spherical and homogeneous in composi-





tion.

190

195

#### 2.5 UKESM1.1 model simulations

Simulations were performed with the atmosphere-only configuration of the model (UKESM1.1-AMIP) and run for a period of 11 years, from January 2004 to December 2014. The first 12 months were discarded as spin-up and we focus our analysis on the 10 years from January 2005 to December 2014. Microplastic emissions for the 12 months of available data have been repeated for each year of the simulations. While this predates atmospheric microplastic observations and the emissions inventory it provides a well tested simulation period for analysis (Mulcahy et al., 2023). Three simulations were performed: A control with no microplastic emissions, one with microplastic fragment emissions and one with microplastic fibre emissions.

## 2.6 Microplastic observations for model evaluation

An examination of existing studies reporting atmospheric microplastic concentrations was undertaken to provide comparison with model output. Published airborne microplastic data was gathered through a Scopus search using the following criteria: (1) search by 'Article Title', (2) search documents 'microplastics AND airborne OR atmospheric OR atmosphere' (3) including all available years. All papers were screened for relevance by reviewing abstracts, with studies excluded if they did not directly measure airborne microplastics and report results in either 'particles m<sup>-3</sup>' or 'particles m<sup>-2</sup> day<sup>-1</sup>'. Relevant studies were then examined in detail to extract key information. While this approach aimed to compile a comprehensive dataset of airborne microplastics to date, it is acknowledged that some relevant studies may not have been captured due to the specific search terms used.

## 3 Results and discussion

## 3.1 Microplastic surface concentrations

Figure 2 shows the annual mean surface concentration from UKESM1.1-AMIP output (2005–2014) for microplastic fragments and fibres. Figure 2a-b shows the microplastic surface number concentration and Figure 2c-d shows the microplastic surface mass concentration. Microplastics have greater number and mass concentrations over land than the ocean, which matches well with the emissions profile (Figure 1). Model output shows that microplastic fragments do not stay localised to their point of emissions, but are advected around the atmosphere such that they are ubiquitous across the globe. For example, over Antarctica small amounts of microplastic are present despite a lack of emissions there for both fragments and fibres. Microplastic fibres (Figure 2b,d) display high concentrations close to areas of population where they are emitted. Fibres display some atmospheric



210



transport into other regions, particularly over coastal regions which are close to emission sources.

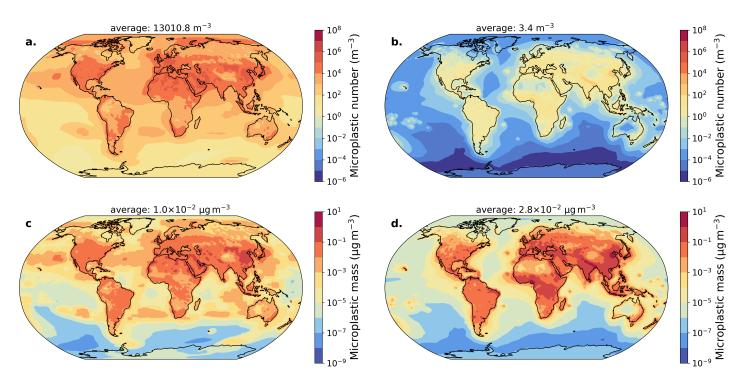


**Figure 2.** Annual-mean surface concentration of microplastics in UKESM1.1-AMIP (2005–2014) for (a) fragment number concentration, (b) fibre number concentration, (c) fragment mass concentration, and (d) fibre mass concentration. The area weighted average is displayed on each subplot.

Figure 2 indicates differences between microplastic fragments and fibres in terms of their surface number and mass concentrations. Microplastic fragments (Figure 2a,c) exhibit a significantly higher surface number concentration  $(1.3 \times 10^4 \text{ m}^{-3})$  compared to microplastic fibres  $(3.4 \text{ m}^{-3})$ . This difference arises because fibres are only represented in the largest size mode (super-coarse insoluble), which contains the fewest microplastic particles. Microplastic fibres contribute slightly more to the surface mass concentration  $(2.8 \times 10^{-2} \text{ µg m}^{-3})$  than microplastic fragments  $(1.0 \times 10^{-2} \text{ µg m}^{-3})$ .

Table 2 presents the average number and mass concentrations of microplastic fragments and fibres across individual size modes, indicating their relative contributions to the total concentrations on Figure 2. The spatial distribution of these concentrations is shown in Supplementary Figures A2-A5. Table 2 indicates fewer microplastics are present at the surface in the soluble modes as compared to the insoluble ones, as microplastics only enter the soluble modes via the build up of soluble material on their surfaces as they age. Ageing does not occur in the super-coarse insoluble mode in the model as there is no





corresponding soluble mode.

220

225

Size Mode	Fragi	ments	Fib	ores
	number (m <sup>-3</sup> )	mass ( $\mu g m^{-3}$ )	number (m <sup>-3</sup> )	mass ( $\mu g m^{-3}$ )
Aitken Insoluble	7410.9	$1.5 \times 10^{-8}$	-	-
Aitken Soluble	3083.6	$6.4 \times 10^{-9}$	-	-
Accumulation Insoluble	1247.7	$2.6 \times 10^{-6}$	-	-
Accumulation Soluble	1075.4	$2.2 \times 10^{-6}$	-	-
Coarse Insoluble	151.7	$1.1 \times 10^{-4}$	-	-
Coarse Soluble	40.3	$2.9 \times 10^{-5}$	-	-
Super-Coarse Insoluble	1.2	$9.9\times10^{-3}$	3.4	$2.8\times10^{-2}$
Total	$1.3 \times 10^4$	$1.0 \times 10^{-2}$	3.4	$2.8 \times 10^{-2}$

**Table 2.** Global annual mean surface number and mass concentrations of microplastic fragments and microplastic fibres across GLOMAP aerosol size modes in UKESM1.1-AMIP.

Microplastic surface number and mass concentrations vary substantially across size modes, as expected from the prescribed size distribution of emissions (Supplementary Figure A1). The highest number concentrations are observed in the Aitken mode and the highest mass concentrations are observed in the super-coarse insoluble mode. Fragments are present in all size modes, with the majority of number concentration in the Aitken insoluble (7410.9 m<sup>-3</sup>) and Aitken soluble (3083.6 m<sup>-3</sup>) modes, highlighting their abundance at the smallest aerosol size of 5 - 50 nm. Fragment surface mass concentration is dominated by the super-coarse insoluble mode ( $9.9 \times 10^{-3} \mu g m^{-3}$ ), despite its small number concentration ( $1.2 m^{-3}$ ). Fibres, which are only allowed in the super-coarse insoluble mode, show greater number ( $3.4 m^{-3}$ ) and mass ( $2.8 \times 10^{-2} \mu g m^{-3}$ ) concentrations compared to microplastic fragments.

Supplementary Figures A2-A4 indicate that soluble modes show a better atmospheric mixing of microplastics compared to the insoluble modes. Supplementary Figure A4 displays a narrower range of microplastic concentrations and smoother spatial distributions observed for soluble particles. In contrast, Supplementary Figures A2,A3 for insoluble microplastics have more varied spatial patterns, with localized regions of elevated concentrations from features such as orography more pronounced.

A previous microplastic modelling study by Revell et al. (2021) assumed a uniform surface microplastic concentration of 1 m<sup>-3</sup>, based on previously reported airborne microplastic concentrations. These studies focused on particle sizes down to 5 μm corresponding to the supercoarse mode used in our study. We show that modelled microplastic surface concentrations for supercoarse-mode particles are 1.2 m<sup>-3</sup> for fragments and 3.4 m<sup>-3</sup> for fibres (Table 2). These concentrations are in the same



245

250

255

260

265



order of magnitude as the assumption of Revell et al. (2021), and suggests that emissions based on Evangeliou et al. (2022) and our modelling approach is consistent with previous research.

# 3.2 Microplastic vertical distributions

Figure 3 shows the vertical profile of microplastic fragments, for each of the four insoluble modes. Microplastic number concentration is averaged over time and longitude to determine the annual zonal mean. Number concentrations of less than 1 m $^{-3}$  are masked out to remove unrealistic values. Microplastics in the Aitken insoluble mode (Figure 3a) show the greatest vertical extent as they are the lightest. They potentially reach altitudes of up to  $\sim$ 17 km at the equator, and  $\sim$ 11 km at the poles. This indicates the lightest insoluble microplastics are well-mixed in the troposphere. A few microplastics are also present in the stratosphere, but do not enter in any great number. The vertical distribution of microplastic influences their radiative effects, as particles suspended higher in the atmosphere have a greater potential to interact with incoming and outgoing radiation. Revell et al. (2021) show that longwave radiative heating by microplastics are larger when microplastics are distributed throughout the troposphere compared to when they are confined to the boundary layer (lowermost 2 km of the atmosphere). Figures 3b-d for the accumulation, coarse, and super-coarse modes show microplastics in these modes are both less numerous and have a lesser vertical extent than the Aitken insoluble mode. The super-coarse insoluble microplastics are mostly confined to the near-surface atmosphere.

Zonal mean microplastic fragment number concentrations at UKESM1.1-AMIP vertical levels for the three microplastic-enabled soluble modes and microplastic fibres are shown on Figure 4. Soluble microplastics show greater vertical extent and higher concentrations than their insoluble mode counterparts (Figure 3), even though the surface number concentration of soluble mode microplastics is less than insoluble mode microplastics (Supplementary Figure A3 and Supplementary Figure A4a,c,e). Figure 4a,b indicates that Aitken/accumulation soluble mode microplastics can be transported to even higher altitudes than insoluble mode microplastics – over 19 km at the equator, reducing towards the poles. This suggests that Aitken and accumulation soluble microplastic fragments are well-mixed in the troposphere and have greater concentrations in the stratosphere than the small insoluble microplastics. They also reach cloud forming altitudes where they may impact cloud formation through their role as CCN (and potentially INP, although this is not yet enabled in the model). Coarse mode soluble microplastics undergo less vertical transport, reaching altitudes of up to ~12.5 km. Figure 4d shows vertical profiles of number concentration for microplastic fibres. Due to their large size they do not reach heights greater than 3 km and are mostly contained near the surface, which can be explained due to their shape being assumed as spherical. The limitations of this approach are discussed below.

Results shown across Figures 3,4 agree with previous work (Tatsii et al., 2024; Bucci et al., 2024) modelling the vertical transport of microplastics, which also found that microplastics reach into the stratosphere. Tatsii et al. (2024) suggested that due to their reduced settling velocities, microplastic fibres ascend higher in the atmosphere and have increased global atmo-





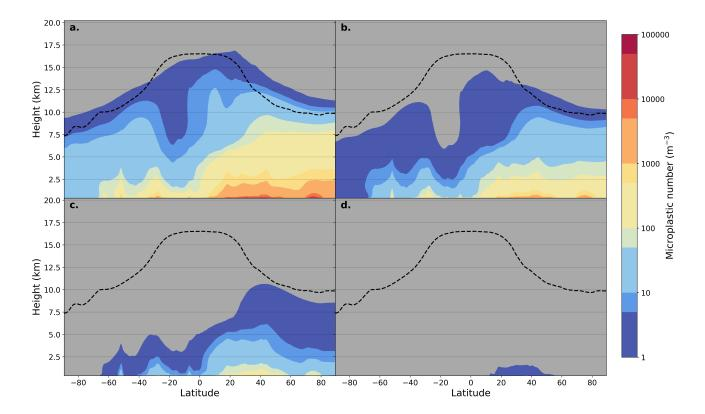


Figure 3. Vertical profile of annual zonal mean microplastic fragment concentration (2005–2014) for (a) Aitken insoluble, (b) accumulation insoluble, (c) coarse insoluble, and (d) super-coarse insoluble modes. Grey shading indicates number concentrations smaller than  $1 \text{ m}^{-3}$ . The dashed line indicates the model's annual-mean tropopause height.

spheric transport than equivalent sized microplastic fragments. As microplastic fibres are currently treated as spherical within the model, this vertical uplift is not seen in Figure 4d and highlights the need for improvements in the representation of mi275 croplastic fibres in future iterations of the microplastic scheme.





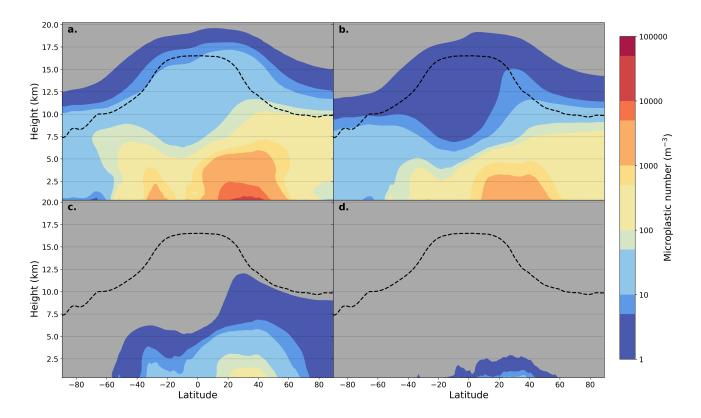


Figure 4. Vertical profile of annual zonal mean microplastic fragment concentrations (2005–2014) for (a) Aitken soluble, (b) accumulation soluble, (c) coarse soluble modes, and (d) super-coarse insoluble microplastic fibres. Grey shading indicates number concentrations smaller than 1  $m^{-3}$ . The dashed line indicates the model's annual-mean tropopause height.

### 3.3 Microplastic burden, loss and lifetime

280

Table 3 shows the global mean microplastic atmospheric burden, deposition processes, and estimated atmospheric lifetime across GLOMAP aerosol size modes in UKESM1.1-AMIP. The total atmospheric burden of microplastic is 600 tonnes, with an estimated mean lifetime of 0.05 days (1.2 hours) before deposition. The burden and lifetime varies substantially across size modes, with the total global microplastic deposition and burden strongly weighted towards the largest super-coarse mode microplastics.

Microplastic removal is dominated by dry deposition across all size modes, though wet deposition pathways indicate some interactions with cloud processes. Soluble mode microplastics show greater loss through wet deposition processes compared to the insoluble size modes. Accumulation soluble mode microplastics show the greatest loss through wet deposition. This reflects the ability of accumulation soluble mode microplastics to become incorporated into cloud droplets as CCN before wet deposition removes them. Atmospheric lifetimes are longer for smaller particles as expected (Seinfeld and Pandis, 2016), with



290

295

305



Size Mode		Loss (tonnes/year)		Burden (tonnes)	Lifetime (days)
	Dry Deposition	Impaction Scavenging	<b>Nucleation Scavenging</b>		
Aitken Insoluble Fragments	0.021 (93.6%)	0.001 (4.6%)	0.0004 (1.8%)	0.00019	3.06
Aitken Soluble Fragments	0.01 (77.3%)	0.0016 (11.6%)	0.0015 (11.1%)	0.00064	17.15
Accumulation Insoluble Fragments	2.51 (95.8%)	0.11 (4.2%)	0 (0%)	0.034	4.6
Accumulation Soluble Fragments	2.62 (38.8%)	0.70 (10.3%)	3.44 (50.9%)	0.2	10.8
Coarse Insoluble Fragments	215 (88.9%)	26.8 (11.1%)	0 (0%)	2.00	3.0
Coarse Soluble Fragments	164 (67.6%)	33.1 (13.6%)	45.7 (18.8%)	2.96	4.4
Super-Coarse Insoluble Fragments	800590 (98.8%)	9912 (1.2%)	0.00 (0%)	295	0.13
Super-Coarse Insoluble Fibres	3520823 (99.2%)	29906 (0.8%)	0.00 (0%)	300	0.03
Total	4321798 (99.1%)	39879 (0.9%)	49.1 (0.001%)	600	0.05

**Table 3.** Global annual mean microplastic (fragments and fibres) aerosol budget showing deposition processes, burden in tonnes (1 tonne = 1000 kg), and lifetime across GLOMAP aerosol size modes in UKESM1.1-AMIP. Wet deposition can be calculated here as the sum of impaction scavenging (washout) and nucleation scavenging (rainout). Percentages indicate the total fraction of loss that each pathway is responsible for within each size mode. Fibres are only present in the super-coarse insoluble mode.

the greatest atmospheric lifetime occurring in the Aitken soluble mode (17.15 days).

Supplementary Table A1 presents the deposition fluxes of microplastics across different size modes as in Table 3, but partitioned between land and ocean. For smaller microplastics, deposition occurs preferentially over land, with Aitken and accumulation mode microplastics exhibiting the highest land-to-ocean deposition ratios. In contrast, larger microplastic modes show greater deposition occurring over the ocean.

The more diffuse spatial patterns and better atmospheric mixing for soluble microplastics (Figures A2-A4) and greater atmospheric lifetimes (Table 3)potentially highlights the ability of soluble microplastics to be incorporated into clouds and water vapour, after which they are carried with the subsequent atmospheric movement. This enables them to travel longer distances, especially if they are embedded in large weather systems like cyclones or fronts (Ryan et al., 2023).

# 300 3.4 Comparison with total aerosol concentration

Table 4 compares present-day microplastic concentrations relative to the total aerosol concentrations within UKESM1.1-AMIP. Across all size modes, microplastics represent a minor percentage of the total aerosol number concentration, with total microplastic particles comprising 0.0005% of the total atmospheric aerosol number concentration. The greatest relative contribution occurs within the super-coarse insoluble mode, where microplastics account for 0.0407% of total aerosol particles. This higher percentage likely reflects the number of other represented super-coarse mode aerosols in GLOMAP, which is currently limited to super-coarse insoluble mode dust (see Table 1).



310

315

320

325



Size Mode	Microplastics (m <sup>-3</sup> )	Total Aerosol (m <sup>-3</sup> )	<b>Percent</b> (10 <sup>-3</sup> %)
Aitken Insoluble	361	$1.41 \times 10^7$	2.6
Aitken Soluble	641	$2.21 \times 10^{8}$	0.3
Accumulation Insoluble	62.9	$1.08 \times 10^{6}$	5.8
Accumulation Soluble	212	$4.47 \times 10^7$	0.5
Coarse Insoluble	9.11	$1.64 \times 10^5$	5.6
Coarse Soluble	8.70	$2.89 \times 10^5$	0.3
Super-Coarse Insoluble	0.24	581	40.7
Total	~1295	$\sim 2.8 \times 10^8$	0.5

**Table 4.** Global annual-mean number concentrations of microplastic (fragments and fibres combined) and total aerosol particles (m<sup>-3</sup>) across GLOMAP aerosol size modes in UKESM1.1-AMIP. The percentage that microplastic contribute to total aerosol is also displayed.

The insoluble percentage of Aitken, accumulation, and coarse mode microplastics display slightly higher relative contributions to total aerosol than their soluble counterparts. This results from the lower number of aerosol species represented in the insoluble modes (see Table 1) and leads to a greater proportional influence of microplastic particles, which are only emitted into the insoluble modes. However, even in these cases, microplastic number concentrations remain orders of magnitude lower than the total aerosol concentration, suggesting that their direct influence on aerosol number concentrations and CCN formation is likely minimal at current concentrations. This is reinforced by Supplementary Figure A6, which shows spatial patterns and differences between microplastic and the control simulations for aerosol optical depth (AOD), CCN, and cloud droplet number concentration (CDNC). Spatial patterns remain consistent across the simulations, with only minor regional variations compared to the control. Only a few isolated regions exhibit statistically significant changes, which are inconsistent across the spatial patterns for AOD, CCN and CDNC.

### 3.5 Comparison with observations

To evaluate model performance, the observational dataset described in Section 2.6 is divided into two categories: active sampling studies reporting atmospheric microplastic number concentrations, and deposition studies reporting microplastic deposition fluxes. We note some difficulties with this approach due to both the limited observations and the lack of standardisation across current observation methods; for sample collection, sample preparation and sample analysis. Observations are compared to the corresponding UKESM1.1-AMIP output by selecting the nearest model grid cell in both latitude and longitude to allow for the best comparison. Because many of the observation studies have detection limits down to  $\sim$ 2  $\mu$ m, only model output corresponding to the super-coarse mode (fragments and fibres combined) is assessed. Figure 5 shows a spatial map of the available observational data for both active sampling and deposition, and a comparison with UKESM1.1-AMIP output. The





comparison between the observations and model output is separated between land and ocean, although reported correlation coefficient (r) values and root mean square error (RMSE) values are for land and ocean combined.

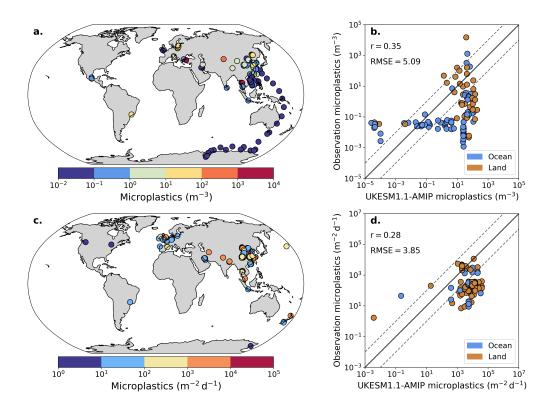


**Figure 5.** (a) Available observational microplastic number concentrations from active sampling studies (b) Comparison of observed concentrations from (a) with UKESM1.1-AMIP surface microplastic number concentrations at the nearest model grid cell (c) Available observational microplastic deposition fluxes from deposition studies (d) Comparison of observed deposition fluxes from (c) with UKESM1.1-AMIP microplastic deposition rates (combined wet and dry) at the nearest model grid cell. The correlation coefficients (r) and root mean square errors (RMSE) across (b) and (d) are calculated in log space, for the ocean and land measurements combined. The 1:1 (solid) and 1:10/10:1 (dashed) lines are plotted on (b) and (d) for reference.

For active sampling studies, Figure 5a shows a regional bias with most studies undertaken in Europe and Asia. The model generally simulates greater microplastic concentrations than the observations, often by a few orders of magnitude, and with a poor correlation coefficient of r = 0.35 and RMSE of 5.09 (Figure 5b). This is particularly evident across studies reporting low observed concentrations, where the model simulates a large range of microplastic concentrations. However the majority of these studies are sampled over the ocean during a single observational study by Chen et al. (2023), and may not be representative of the microplastic concentration. Figure 5c also shows that the observations of microplastic deposition are biased towards European and Asian locations. Comparisons with the model shows slightly lower correlation coefficient of r = 0.28,





but a reduced RMSE of 3.85 (Figure 5d).

The disagreement between the model and observations is unsurprising, as observations represent a point source while the model output is the average over each latitude/longitude grid cell. Regions of high spatial variability such as around urban population centres would be most impacted by this discrepancy. Furthermore, many of the observational studies to date used micro-Fourier Transform Infrared Spectroscopy (µFTIR), which can only analyse microplastics of diameter 11 µm and larger (Allen et al., 2022), i.e. it cannot resolve microplastics down to the 2.5 µm threshold of the UKESM1.1 super-coarse mode (Table 2). This also accounts for some of the differences between the observations and the model.

### 4 Conclusions

345

350

355

In this study, we introduced atmospheric microplastic as an aerosol species into UKESM1.1, then presented results of global microplastic concentration and deposition by running UKESM1.1 in an atmosphere only configuration. Assessing the vertical transport of microplastics indicates that the smaller microplastics are well mixed in the troposphere, with some microplastics also reaching the stratosphere in small numbers (Figures 3,4).

The representation of microplastics in UKESM1.1 has high levels of uncertainty, largely due to the limited available of observational data, both going into the emissions used in the model and for comparison with model output. The input of microplastics into climate models will require constant updating as our understanding of airborne microplastics increases, through both increased sampling with good global coverage and the standardisation of collection and and analysis methodology. Another large source of model uncertainty is the currently representation of microplastic fibres which are assumed to be spherical. Fibres need to be treated as non-spherical particles with different settling velocities to microplastic fragments due to their shape (Tatsii et al., 2024). Future iterations of the microplastics scheme will seek to incorporate better emissions estimates and improve the representation of microplastic fibres.

Compared to total aerosol number concentrations, microplastics currently contribute a minor fraction (Table 4). With global plastic production projected to increase substantially over the coming decades (Geyer et al., 2017), microplastic emissions and consequently their contribution to atmospheric aerosol concentrations are expected to grow. This is particularly relevant in regions influenced by strong sources of microplastics such as population centres which contribute through tyre-wear particles and microplastic fibres from textiles.

The incorporation of microplastics into UKESM1.1 provides a crucial step toward quantifying their present atmospheric burdens and understanding their impact on the climate. It also paves the way for future studies assessing human exposure to microplastics. The ability to simulate future emission scenarios of microplastics with UKESM1.1 allows for assessment of

**17** 

360

365





370 long-term impacts, highlighting the importance of including microplastics in Earth system models as plastic pollution continues to escalate.

*Code and data availability.* Due to intellectual property rights restrictions, we cannot provide either the source code or documentation papers for the UM. The data used to produce the figures and tables is available at https://doi.org/10.5281/zenodo.15127661 (McErlich, 2025).

375 Appendix A





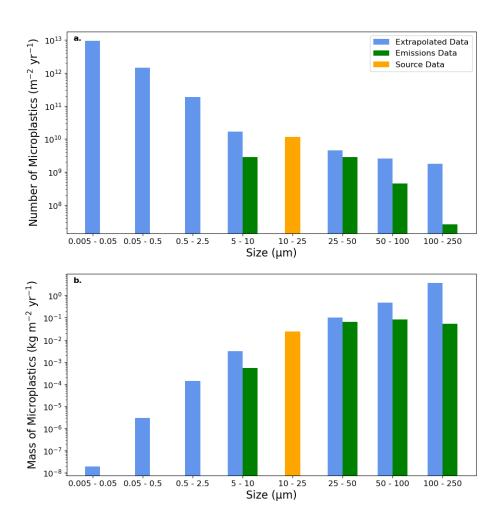


**Figure A1.** Microplastic emissions extrapolated across varying size bins for (a) number concentration and (b) mass concentration. Green bars represent reference emissions data from (Evangeliou et al., 2022). The orange bar indicates the bin from which emissions were extrapolated for input to the model (blue bars).



## Insoluble modes: mass concentration

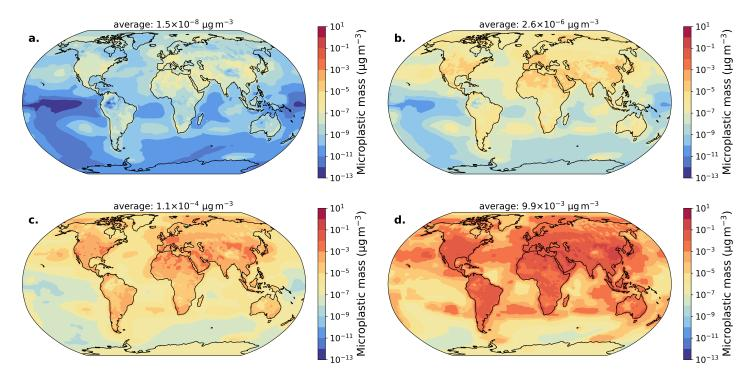


**Figure A2.** Annual-mean surface mass concentration of microplastic fragments in UKESM1.1-AMIP (2005–2014) for (a) Aitken, (b) accumulation, (c) coarse, and (d) super-coarse insoluble modes. The global-, area weighted average is displayed on each subplot.





# Insoluble modes: number concentration

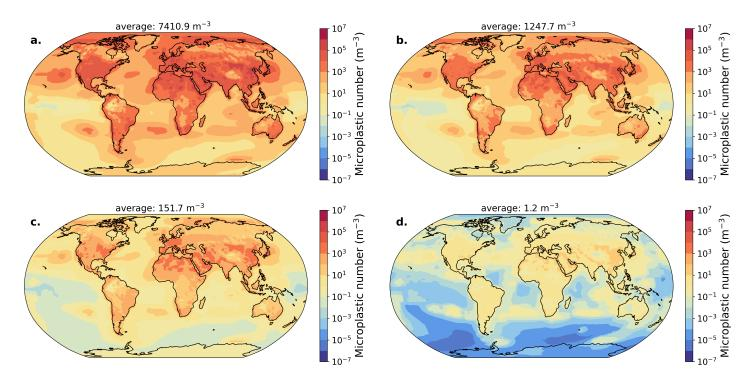
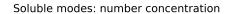


Figure A3. As for Figure A2, but showing microplastic number concentrations.







# Soluble modes: mass concentration

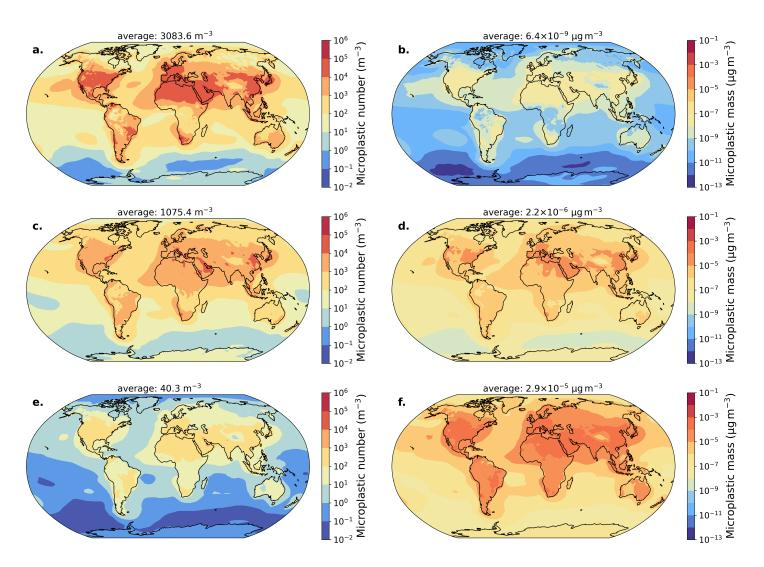


**Figure A4.** Annual-mean surface number concentration of microplastic fragments in UKESM1.1-AMIP (2005–2014) for (a) Aitken soluble mode number (b) Aitken soluble mode mass (c) accumulation soluble mode number (d) accumulation soluble mode mass (e) coarse soluble mode number (f) coarse soluble mode mass. The global-, area weighted average is displayed on each subplot.





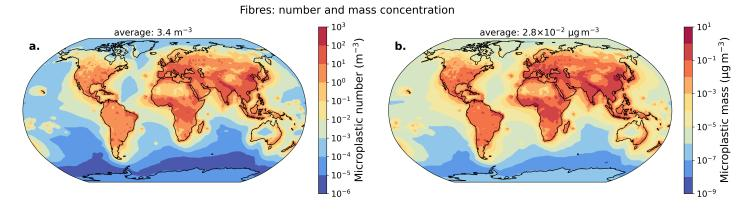


**Figure A5.** Annual surface concentrations of microplastic fibres in UKESM1.1-AMIP (2005–2014) for (a) super-coarse insoluble mode number and (b) mass. The global, area-weighted average is displayed on each subplot.





Size Mode	Dry Depositi	Dry Deposition (tonnes/yr)	Impaction Scaven	Impaction Scavenging (tonnes/yr)	Nucleation Scavenging (tonnes/yr)	inging (tonnes/yr)	Total Deposition (tonnes/yr)	on (tonnes/yr)
	Land	Ocean	Land	Ocean	Land	Ocean	Land	Ocean
Aitken	0.0229 (73.2%)	0.0084 (26.8%)	0.0021 (79.7%)	0.0005 (20.3%)	0.0005 (20.3%) 0.0014 (75.4%) 0.0005 (24.6%)	0.0005 (24.6%)	0.0264 (73.8%)	0.0094 (26.2%)
Accumulation	3.79 (73.8%)	1.35 (26.2%)	0.642 (79.5%)	0.166 (20.5%)	2.69 (78.2%)	0.751 (21.8%)	7.12 (75.9%)	2.26 (24.1%)
Coarse	265.25 (70.0%)	113.69 (30.0%)	51.43 (85.8%)	8.51 (14.2%)	34.86 (76.3%)	10.84 (23.7%)	351.54 (72.6%)	133.04 (27.4%)
Supercoarse	549475.7 (68.6%)	251114.7 (31.4%)	9194.14 (92.8%)	717.57 (7.2%)	0.00 (0.0%)	0.00 (0.0%)	558669.8 (68.9%)	251832.3 (31.1%)
Fibres	2039073.0 (57.9%)	$ \begin{array}{c ccccccccccccccccccccccccccccccccccc$	24723.67 (82.7%)	5182.80 (17.3%)	0.00 (0.0%)	0.00 (0.0%)	2063797.0  (58.1%)  1486932.0  (41.9%)	1486932.0 (41.9%)
Total	2588818 (59.9%)	2588818 (59.9%) 1732980 (40.1%)	33970 (85.2%)	5909 (14.8%)	37.55 (76.4%)	12.59 (23.6%)	5909 (14.8%) 37.55 (76.4%) 12.59 (23.6%) 2622825 (60.1%) 1738900 (39.9%)	1738900 (39.9%)
Table A 1 Dens	Toble A1 Describing of winner of winner of winner thousandrones for another man down and and and and and and and	(1) (4) (4) (1) (1) (1) (1) (1)	on) for sook domesti	- 7	orthogon objects on:	- Caro Lond acres to	Donotanto	adiante the function

Table A1. Deposition fluxes of microplastic (tonnes/year) for each deposition process and size mode, masked over land and ocean. Percentages indicate the fraction





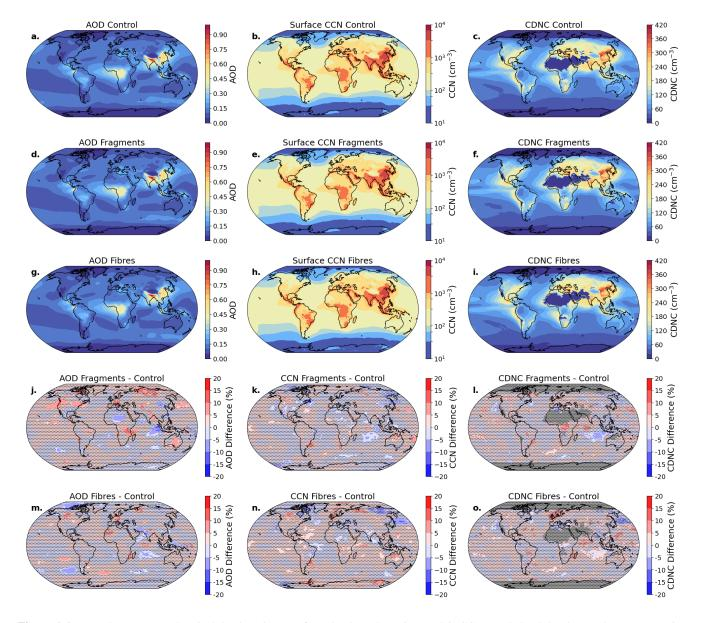


**Figure A6.** Annual mean aerosol optical depth (AOD), surface cloud condensation nuclei (CCN), and cloud droplet number concentration (CDNC) from UKESM1.1-AMIP (2005–2014) for microplastic fragments, fibres, and the control simulation. (a-c) AOD, CCN, and CDNC for the control simulation without microplastics respectively (d-f) same as (a-c) but for microplastic fragments (g-i) same as (a-c) but for microplastic fibres (j-i) show the percentage difference between the microplastic fragments and control simulations for each variable. (m-o) same as (j-i) but for microplastic fibres and control simulations. Stippling in the difference plots indicates areas where changes are not statistically significant at the 95% confidence level.





Author contributions. CM developed the microplastics scheme, with assistance from FG. CM performed the simulations and analysis, with assistance from LER and CH. AA provided the observational data. NE provided the microplastics emissions inventory. CM wrote the manuscript with assistance from all co-authors.

Competing interests. The authors declare they have no competing interests.

Acknowledgements. This research was supported by the Royal Society Te Apārangi Marsden Fund (22-UOC-088). We acknowledge the UK Met Office for the use of the UKESM1.1. We also acknowledge the contribution of NeSI high-performance computing facilities to the results of this research. New Zealand's national facilities are provided by NeSI and funded jointly by NeSI's collaborator institutions and through the Ministry of Business, Innovation and Employment's Research Infrastructure programme (https://www.nesi.org.nz/). LER appreciates support by the Rutherford Discovery Fellowships from New Zealand Government funding, administered by the Royal Society Te Apārangi.

NE was funded by the Norwegian Research Council (NFR) project MAGIC (Airborne Microplastic Detection, Origin, Transport and Global





#### References

- Abdul-Razzak, H. and Ghan, S. J.: A parameterization of aerosol activation: 2. Multiple aerosol types, Journal of Geophysical Research: Atmospheres, 105, 6837–6844, https://doi.org/10.1029/1999JD901161, 2000.
- Aeschlimann, M., Li, G., Kanji, Z. A., and Mitrano, D. M.: Potential impacts of atmospheric microplastics and nanoplastics on cloud formation processes, Nature Geoscience, 15, 967–975, https://doi.org/10.1038/s41561-022-01051-9, 2022.
  - Albrecht, B. A.: Aerosols, Cloud Microphysics, and Fractional Cloudiness, Science, 245, 1227–1230, https://doi.org/10.1126/science.245.4923.1227, 1989.
- Allen, D., Allen, S., Abbasi, S., Baker, A., Bergmann, M., Brahney, J., Butler, T., Duce, R. A., Eckhardt, S., Evangeliou, N., Jickells, T.,

  Kanakidou, M., Kershaw, P., Laj, P., Levermore, J., Li, D., Liss, P., Liu, K., Mahowald, N., Masque, P., Materić, D., Mayes, A. G.,

  McGinnity, P., Osvath, I., Prather, K. A., Prospero, J. M., Revell, L. E., Sander, S. G., Shim, W. J., Slade, J., Stein, A., Tarasova, O., and

  Wright, S.: Microplastics and nanoplastics in the marine-atmosphere environment, Nature Reviews Earth & Environment, 3, 393–405,

  https://doi.org/10.1038/s43017-022-00292-x, 2022.
- Allen, S., Allen, D., Baladima, F., Phoenix, V. R., Thomas, J. L., Le Roux, G., and Sonke, J. E.: Evidence of free tropospheric and long-range transport of microplastic at Pic du Midi Observatory, Nature Communications, 12, 7242, https://doi.org/10.1038/s41467-021-27454-7, 2021.
  - Archibald, A. T., O'Connor, F. M., Abraham, N. L., Archer-Nicholls, S., Chipperfield, M. P., Dalvi, M., Folberth, G. A., Dennison, F., Dhomse, S. S., Griffiths, P. T., Hardacre, C., Hewitt, A. J., Hill, R. S., Johnson, C. E., Keeble, J., Köhler, M. O., Morgenstern, O., Mulcahy, J. P., Ordóñez, C., Pope, R. J., Rumbold, S. T., Russo, M. R., Savage, N. H., Sellar, A., Stringer, M., Turnock, S. T., Wild, O.,
- and Zeng, G.: Description and evaluation of the UKCA stratosphere–troposphere chemistry scheme (StratTrop vn 1.0) implemented in UKESM1, Geoscientific Model Development, 13, 1223–1266, https://doi.org/10.5194/gmd-13-1223-2020, 2020.
  - Aves, A. R., Revell, L. E., Gaw, S., Ruffell, H., Schuddeboom, A., Wotherspoon, N. E., LaRue, M., and McDonald, A. J.: First evidence of microplastics in Antarctic snow, The Cryosphere, 16, 2127–2145, https://doi.org/10.5194/tc-16-2127-2022, 2022.
- Bellouin, N.: Interaction of UKCA aerosols with radiation: UKCA RADAER, Tech. rep., Tech. rep., UK Met Office, available at: http://www. 410 ukca. ac. uk/wiki ..., 2010.
  - Bergmann, M., Mützel, S., Primpke, S., Tekman, M. B., Trachsel, J., and Gerdts, G.: White and wonderful? Microplastics prevail in snow from the Alps to the Arctic, Science Advances, 5, eaax1157, https://doi.org/10.1126/sciadv.aax1157, 2019.
  - Brahana, P., Zhang, M., Nakouzi, E., and Bharti, B.: Weathering influences the ice nucleation activity of microplastics, Nature Communications, 15, 9579, https://doi.org/10.1038/s41467-024-53987-8, 2024.
- Brahney, J., Hallerud, M., Heim, E., Hahnenberger, M., and Sukumaran, S.: Plastic rain in protected areas of the United States, Science, 368, 1257–1260, https://doi.org/10.1126/science.aaz5819, 2020.
  - Bucci, S., Richon, C., and Bakels, L.: Exploring the Transport Path of Oceanic Microplastics in the Atmosphere, Environmental Science & Technology, 58, 14 338–14 347, https://doi.org/10.1021/acs.est.4c03216, 2024.
- Busse, H. L., Ariyasena, D. D., Orris, J., and Freedman, M. A.: Pristine and Aged Microplastics Can Nucleate Ice through Immersion 420 Freezing, ACS ES&T Air, https://doi.org/10.1021/acsestair.4c00146, 2024.
  - Carpenter, E. J. and Smith, K. L.: Plastics on the Sargasso Sea Surface, Science, 175, 1240–1241, https://doi.org/10.1126/science.175.4027.1240, 1972.



435

455



- Carpenter, E. J., Anderson, S. J., Harvey, G. R., Miklas, H. P., and Peck, B. B.: Polystyrene Spherules in Coastal Waters, Science, 178, 749–750, https://doi.org/10.1126/science.178.4062.749, 1972.
- 425 Chen, Q., Shi, G., Revell, L. E., Zhang, J., Zuo, C., Wang, D., Le Ru, E. C., Wu, G., and Mitrano, D. M.: Long-range atmospheric transport of microplastics across the southern hemisphere, Nature Communications, 14, 7898, https://doi.org/10.1038/s41467-023-43695-0, 2023.
  - Dris, R., Gasperi, J., Rocher, V., Saad, M., Renault, N., and Tassin, B.: Microplastic contamination in an urban area: a case study in Greater Paris, Environmental Chemistry, 12, 592–599, https://doi.org/10.1071/EN14167, 2015.
- Edwards, J. M. and Slingo, A.: Studies with a Flexible New Radiation Code. I: Choosing a Configuration for a Large-Scale Model, Quarterly

  Journal of the Royal Meteorological Society, 122, 689–719, https://doi.org/10.1002/qj.49712253107, 1996.
  - Evangeliou, N., Grythe, H., Klimont, Z., Heyes, C., Eckhardt, S., Lopez-Aparicio, S., and Stohl, A.: Atmospheric transport is a major pathway of microplastics to remote regions, Nature Communications, 11, 3381, https://doi.org/10.1038/s41467-020-17201-9, 2020.
  - Evangeliou, N., Tichý, O., Eckhardt, S., Zwaaftink, C. G., and Brahney, J.: Sources and fate of atmospheric microplastics revealed from inverse and dispersion modelling: From global emissions to deposition, Journal of Hazardous Materials, 432, 128585, https://doi.org/https://doi.org/10.1016/j.jhazmat.2022.128585, 2022.
  - Forster, P., Storelvmo, T., Armour, K., Collins, W., Dufresne, J.-L., Frame, D., Lunt, D., Mauritsen, T., Palmer, M., Watanabe, M., Wild, M., and Zhang, H.: The Earth's Energy Budget, Climate Feedbacks, and Climate Sensitivity, in: Climate Change 2021: The Physical Science Basis. Contribution of Working Group I to the Sixth Assessment Report of the Intergovernmental Panel on Climate Change, edited by Masson-Delmotte, V., Zhai, P., Pirani, A., Connors, S. L., Péan, C., Berger, S., Caud, N., Chen, Y., Goldfarb, L., Gomis, M. I., Huang,
- M., Leitzell, K., Lonnoy, E., Matthews, J. B. R., Maycock, T. K., Waterfield, T., Yelekçi, O., Yu, R., and Zhou, B., book section 7, pp. 923–1054, Cambridge University Press, Cambridge, UK and New York, NY, USA, https://doi.org/10.1017/9781009157896.009, 2021.
  - Ganguly, M. and Ariya, P. A.: Ice Nucleation of Model Nanoplastics and Microplastics: A Novel Synthetic Protocol and the Influence of Particle Capping at Diverse Atmospheric Environments, ACS Earth and Space Chemistry, 3, 1729–1739, https://doi.org/10.1021/acsearthspacechem.9b00132, 2019.
- Gewert, B., Plassmann, M. M., and MacLeod, M.: Pathways for degradation of plastic polymers floating in the marine environment, Environ. Sci.: Processes Impacts, 17, 1513–1521, https://doi.org/10.1039/C5EM00207A, 2015.
  - Geyer, R., Jambeck, J. R., and Law, K. L.: Production, use, and fate of all plastics ever made, Science Advances, 3, e1700782, https://doi.org/10.1126/sciadv.1700782, 2017.
- González-Pleiter, M., Edo, C., Ángeles Aguilera, Viúdez-Moreiras, D., Pulido-Reyes, G., González-Toril, E., Osuna, S., de Diego-Castilla, G., Leganés, F., Fernández-Piñas, F., and Rosal, R.: Occurrence and transport of microplastics sampled within and above the planetary boundary layer, Science of The Total Environment, 761, 143 213, https://doi.org/https://doi.org/10.1016/j.scitotenv.2020.143213, 2021.
  - Isobe, A., Azuma, T., Cordova, M. R., Cózar, A., Galgani, F., Hagita, R., Kanhai, L. D., Imai, K., Iwasaki, S., Kako, S., Kozlovskii, N., Lusher, A. L., Mason, S. A., Michida, Y., Mituhasi, T., Morii, Y., Mukai, T., Popova, A., Shimizu, K., Tokai, T., Uchida, K., Yagi, M., and Zhang, W.: A Multilevel Dataset of Microplastic Abundance in the World's Upper Ocean and the Laurentian Great Lakes, Microplastics and Nanoplastics, 1, 16, https://doi.org/10.1186/s43591-021-00013-z, 2021.
  - Jones, A. C., Hill, A., Remy, S., Abraham, N. L., Dalvi, M., Hardacre, C., Hewitt, A. J., Johnson, B., Mulcahy, J. P., and Turnock, S. T.: Exploring the sensitivity of atmospheric nitrate concentrations to nitric acid uptake rate using the Met Office's Unified Model, Atmospheric Chemistry and Physics, 21, 15 901–15 927, https://doi.org/10.5194/acp-21-15901-2021, 2021.
- Kvale, K., Prowe, A. E. F., Chien, C.-T., Landolfi, A., and Oschlies, A.: Zooplankton grazing of microplastic can accelerate global loss of ocean oxygen, Nature Communications, 12, 2358, https://doi.org/10.1038/s41467-021-22554-w, 2021.



475

480

485

490



- Leusch, F. D., Lu, H.-C., Perera, K., Neale, P. A., and Ziajahromi, S.: Analysis of the literature shows a remarkably consistent relationship between size and abundance of microplastics across different environmental matrices, Environmental Pollution, 319, 120 984, https://doi.org/https://doi.org/10.1016/j.envpol.2022.120984, 2023.
- MacLeod, M., Arp, H. P. H., Tekman, M. B., and Jahnke, A.: The global threat from plastic pollution, Science, 373, 61–65, https://doi.org/10.1126/science.abg5433, 2021.
  - Mann, G. W., Carslaw, K. S., Spracklen, D. V., Ridley, D. A., Manktelow, P. T., Chipperfield, M. P., Pickering, S. J., and Johnson, C. E.: Description and evaluation of GLOMAP-mode: a modal global aerosol microphysics model for the UKCA composition-climate model, Geoscientific Model Development, 3, 519–551, https://doi.org/10.5194/gmd-3-519-2010, 2010.
- Materić, D., Ludewig, E., Brunner, D., Röckmann, T., and Holzinger, R.: Nanoplastics transport to the remote, high-altitude Alps, Environmental Pollution, 288, 117 697, https://doi.org/10.1016/j.envpol.2021.117697, 2021.
  - McErlich, C.: Microplastic Modelling: April 14th, 2025 release (Version 1.2) [Dataset], https://doi.org/10.5281/zenodo.15207702, 2025.
  - Mulcahy, J. P., Jones, C., Sellar, A., Johnson, B., Boutle, I. A., Jones, A., Andrews, T., Rumbold, S. T., Mollard, J., Bellouin, N., Johnson, C. E., Williams, K. D., Grosvenor, D. P., and McCoy, D. T.: Improved Aerosol Processes and Effective Radiative Forcing in HadGEM3 and UKESM1, Journal of Advances in Modeling Earth Systems, 10, 2786–2805, https://doi.org/https://doi.org/10.1029/2018MS001464, 2018.
  - Mulcahy, J. P., Johnson, C., Jones, C. G., Povey, A. C., Scott, C. E., Sellar, A., Turnock, S. T., Woodhouse, M. T., Abraham, N. L., Andrews, M. B., Bellouin, N., Browse, J., Carslaw, K. S., Dalvi, M., Folberth, G. A., Glover, M., Grosvenor, D. P., Hardacre, C., Hill, R., Johnson, B., Jones, A., Kipling, Z., Mann, G., Mollard, J., O'Connor, F. M., Palmiéri, J., Reddington, C., Rumbold, S. T., Richardson, M., Schutgens, N. A. J., Stier, P., Stringer, M., Tang, Y., Walton, J., Woodward, S., and Yool, A.: Description and evaluation of aerosol in UKESM1 and HadGEM3-GC3.1 CMIP6 historical simulations, Geoscientific Model Development, 13, 6383–6423, https://doi.org/10.5194/gmd-13-6383-2020, 2020.
  - Mulcahy, J. P., Jones, C. G., Rumbold, S. T., Kuhlbrodt, T., Dittus, A. J., Blockley, E. W., Yool, A., Walton, J., Hardacre, C., Andrews, T., Bodas-Salcedo, A., Stringer, M., de Mora, L., Harris, P., Hill, R., Kelley, D., Robertson, E., and Tang, Y.: UKESM1.1: development and evaluation of an updated configuration of the UK Earth System Model, Geoscientific Model Development, 16, 1569–1600, https://doi.org/10.5194/gmd-16-1569-2023, 2023.
  - Revell, L. E., Kuma, P., Le Ru, E. C., Somerville, W. R. C., and Gaw, S.: Direct radiative effects of airborne microplastics, Nature, 598, 462–467, https://doi.org/10.1038/s41586-021-03864-x, 2021.
  - Ryan, A. C., Allen, D., Allen, S., Maselli, V., LeBlanc, A., Kelleher, L., Krause, S., Walker, T. R., and Cohen, M.: Transport and deposition of ocean-sourced microplastic particles by a North Atlantic hurricane, Communications Earth & Environment, 4, 442, https://doi.org/10.1038/s43247-023-01115-7, 2023.
  - Seifried, T. M., Nikkho, S., Morales Murillo, A., Andrew, L. J., Grant, E. R., and Bertram, A. K.: Microplastic Particles Contain Ice Nucleation Sites That Can Be Inhibited by Atmospheric Aging, Environmental Science & Technology, 58, 15711–15721, https://doi.org/10.1021/acs.est.4c02639, 2024.
  - Seinfeld, J. H. and Pandis, S. N.: Atmospheric chemistry and physics: from air pollution to climate change, John Wiley & Sons, 2016.
- Sellar, A. A., Jones, C. G., Mulcahy, J. P., Tang, Y., Yool, A., Wiltshire, A., O'Connor, F. M., Stringer, M., Hill, R., Palmieri, J., Woodward, S., de Mora, L., Kuhlbrodt, T., Rumbold, S. T., Kelley, D. I., Ellis, R., Johnson, C. E., Walton, J., Abraham, N. L., Andrews, M. B., Andrews, T., Archibald, A. T., Berthou, S., Burke, E., Blockley, E., Carslaw, K., Dalvi, M., Edwards, J., Folberth, G. A., Gedney, N., Griffiths, P. T., Harper, A. B., Hendry, M. A., Hewitt, A. J., Johnson, B., Jones, A., Jones, C. D., Keeble, J., Liddicoat, S., Morgenstern,





- O., Parker, R. J., Predoi, V., Robertson, E., Siahaan, A., Smith, R. S., Swaminathan, R., Woodhouse, M. T., Zeng, G., and Zerroukat, M.: UKESM1: Description and Evaluation of the U.K. Earth System Model, Journal of Advances in Modeling Earth Systems, 11, 4513–4558, https://doi.org/https://doi.org/10.1029/2019MS001739, 2019.
  - Tatsii, D., Bucci, S., Bhowmick, T., Guettler, J., Bakels, L., Bagheri, G., and Stohl, A.: Shape Matters: Long-Range Transport of Microplastic Fibers in the Atmosphere, Environmental Science & Technology, 58, 671–682, https://doi.org/10.1021/acs.est.3c08209, 2024.
- Tatsii, D., Gasparini, B., Evangelou, I., Bucci, S., and Stohl, A.: Do Microplastics Contribute to the Total Num-505 ber Concentration of Ice Nucleating Particles?, Journal of Geophysical Research: Atmospheres, 130, e2024JD042827, https://doi.org/https://doi.org/10.1029/2024JD042827, 2025.
  - Twomey, S.: The Influence of Pollution on the Shortwave Albedo of Clouds, Journal of Atmospheric Sciences, 34, 1149 1152, https://doi.org/10.1175/1520-0469(1977)034<1149:TIOPOT>2.0.CO;2, 1977.
- Walters, D., Baran, A. J., Boutle, I., Brooks, M., Earnshaw, P., Edwards, J., Furtado, K., Hill, P., Lock, A., Manners, J., Morcrette, C., Mulcahy,
  J., Sanchez, C., Smith, C., Stratton, R., Tennant, W., Tomassini, L., Van Weverberg, K., Vosper, S., Willett, M., Browse, J., Bushell, A.,
  Carslaw, K., Dalvi, M., Essery, R., Gedney, N., Hardiman, S., Johnson, B., Johnson, C., Jones, A., Jones, C., Mann, G., Milton, S.,
  Rumbold, H., Sellar, A., Ujiie, M., Whitall, M., Williams, K., and Zerroukat, M.: The Met Office Unified Model Global Atmosphere
  7.0/7.1 and JULES Global Land 7.0 configurations, Geoscientific Model Development, 12, 1909–1963, https://doi.org/10.5194/gmd-12-1909-2019, 2019.
- Wang, Y., Okochi, H., Tani, Y., Hayami, H., Minami, Y., Katsumi, N., Takeuchi, M., Sorimachi, A., Fujii, Y., Kajino, M., Adachi, K., Ishihara, Y., Iwamoto, Y., and Niida, Y.: Airborne hydrophilic microplastics in cloud water at high altitudes and their role in cloud formation, Environmental Chemistry Letters, 21, 3055–3062, https://doi.org/10.1007/s10311-023-01626-x, 2023.
  - Xiao, S., Cui, Y., Brahney, J., Mahowald, N. M., and Li, Q.: Long-distance atmospheric transport of microplastic fibres influenced by their shapes, Nature Geoscience, 16, 863–870, https://doi.org/10.1038/s41561-023-01264-6, 2023.
- Xu, X., Li, T., Zhen, J., Jiang, Y., Nie, X., Wang, Y., Yuan, X.-Z., Mao, H., Wang, X., Xue, L., and Chen, J.: Characterization of Microplastics in Clouds over Eastern China, Environmental Science & Technology Letters, 11, 16–22, https://doi.org/10.1021/acs.estlett.3c00729, 2024.